Thymosin-β_4 Changes the Conformation and Dynamics of Actin Monomers

Enrique M. De La Cruz,* E. Michael Ostap,* Rodney A. Brundage,† K. S. Reddy,‡ H. Lee Sweeney,* and Daniel Safer*†

*Pennsylvania Muscle Institute and Department of Physiology, †Department of Cell and Developmental Biology, and ‡Johnson Research Foundation, University of Pennsylvania School of Medicine, Philadelphia, Pennsylvania 19104 USA

ABSTRACT Thymosin-β_4 (Tβ_4) binds actin monomers stoichiometrically and maintains the bulk of the actin monomer pool in metazoan cells. Tβ_4 binding quenches the fluorescence of *N*-iodoacetyl-*N*′-(5-sulfo-1-naphthyl)ethylenediamine (AEDANS) conjugated to Cys^{374} of actin monomers. The K_d of the actin-Tβ_4 complex depends on the cation and nucleotide bound to actin but is not affected by the AEDANS probe. The different stabilities are determined primarily by the rates of dissociation. At 25°C, the free energy of Tβ_4 binding MgATP-actin is primarily enthalpic in origin but entropic for CaATP-actin. Binding is coupled to the dissociation of bound water molecules, which is greater for CaATP-actin than MgATP-actin monomers. Proteolysis of MgATP-actin, but not CaATP-actin, at Gly^{46} on subdomain 2 is >12 times faster when Tβ_4 is bound. The C terminus of Tβ_4 contacts actin near this cleavage site, at His^{40}. By tritium exchange, Tβ_4 slows the exchange rate of approximately eight rapidly exchanging amide protons on actin. We conclude that Tβ_4 changes the conformation and structural dynamics ("breathing") of actin monomers. The conformational change may reflect the unique ability of Tβ_4 to sequester actin monomers and inhibit nucleotide exchange.

INTRODUCTION

Bound nucleotide and divalent cation affect actin monomer assembly, conformation, and interaction with regulatory actin-binding proteins. The monomer sequestering protein, thymosin-β_4 (Tβ_4), forms a 1:1 complex with actin monomers and inhibits polymerization and nucleotide exchange. Tβ_4 has a much greater preference for ATP-actin over ADP-actin monomers (Carlier et al., 1993), so the pool of unpolymerized actin in cells consists of ATP-actin and essentially no ADP-actin.

The majority of quantitative assays for Tβ_4 binding to actin are indirect and rely on changes in the critical concentration (Weber et al., 1992; Hannappel and Wartenberg, 1993; Heintz et al., 1993; Yu et al., 1993; Carlier et al., 1993; Jean et al., 1994; Huff et al., 1995), time courses of actin polymerization (Reichert et al., 1994), nucleotide exchange from actin monomers (Goldschmidt-Clermont et al., 1992), or competition with other actin-binding proteins (Vinson et al., 1998). There are two exceptions in the literature: fluorescence quenching of a bimanyl probe conjugated to Cys^{374} of actin was used to measure the affinity for CaATP-actin monomers (Heintz et al., 1993); and a change in tryptophan fluorescence of actin was used to measure the association and affinity for Ca-ATP- and Mg-ATP-actin monomers (Jean et al., 1994). No direct measurement of dissociation from ATP-actin monomers or binding to ADP-actin has been reported to date.

We initiated this study to 1) evaluate the mechanism, kinetics, affinity, thermodynamics, and nucleotide and cation dependence of Tβ_4 binding to actin monomers, using a direct binding assay; 2) directly measure dissociation of the ATP- and ADP-actin-Tβ_4 complexes; 3) determine if the conformation and dynamics of actin monomers are affected by Tβ_4 binding; and 4) further define the Tβ_4 binding site on actin monomers to resolve two conflicting models in the literature. We have taken advantage of a large change in the fluorescence of *N*-iodoacetyl-*N*′-(5-sulfo-1-naphthyl)ethylenediamine (AEDANS)-actin monomers that accompanies the binding of Tβ_4 to monitor binding. The fluorescence of AEDANS-actin has been used to measure the rates of nucleotide and divalent cation exchange (Frieden et al., 1980) and is therefore sensitive to minor structural rearrangements induced by the occupancy of the nucleotide binding cleft. In addition, we present evidence that Tβ_4 binds subdomain 2 of actin and reduces the breathing movements of monomers. We conclude that Tβ_4 regulates actin assembly and nucleotide exchange through conformational as well as steric effects.

EXPERIMENTAL PROCEDURES

Proteins and reagents

All reagents were of the highest purity available. Rabbit skeletal actin was purified from back and leg muscles (Pardee and Spudich, 1982) and gel-filtered (MacLean-Fletcher and Pollard, 1980) over Sephacryl S300 or Superdex 200 equilibrated in G-buffer (0.2 mM ATP, 0.1 mM $CaCl_2$, 0.5 mM dithiothreitol (DTT), 1 mM NaN_3, 5 mM

Received for publication 7 December 1999 and in final form 2 February 2000.

Address reprint requests to Dr. Enrique M. De La Cruz or Dr. Daniel Safer, Department of Physiology, University of Pennsylvania Medical School, A700 Richards Building, 3700 Hamilton Walk, Philadelphia, PA 19104. Tel.: 215-898-3685; Fax: 215-573-8871; E-mail: enriquem@mail.med.upenn.edu or saferd@mail.med.upenn.edu.

0006-3495/00/05/2516/12 $2.00

imidazole, pH 7.0) at 4°C. The concentration was determined by absorbance, using $\epsilon_{290} = 2.66 \times 10^4\ M^{-1}\ cm^{-1}$ (Houk and Ue, 1974). Actin was labeled at Cys^{374} with AEDANS-iodoacetamide to >98% efficiency, following the protocol for labeling with pyrenyl-iodoacetamide (Pollard, 1984), then gel-filtered. The concentration and extent of labeling were calculated, using $\epsilon_{337} = 6000\ M^{-1}\ cm^{-1}$ and $\epsilon_{290}/\epsilon_{337} = 0.21$ for AEDANS (Lehrer and Kerwar, 1972). MgATP-actin and MgADP-actin monomers were prepared immediately before use as described (Pollard, 1984; Kinosian et al., 1993; Vinson et al., 1998). Tβ_4 was isolated from bovine spleen (Safer et al., 1997).

Construction of S43C-Tβ_4

The cDNA for human Tβ_4 (kindly provided by Drs. C. Panneerselvam and B. L. Horecker of Cornell University) was cloned into pcDNA3 (Invitrogen). Oligonucleotides were designed to add a 5′ *Nde*I site at the initiating methionine and a 3′ *Eco*RI restriction site after the stop codon. In addition, the 3′ oligo contained a mutation that converts the terminal serine residue to a cysteine: TCG to TGT. Cloned products were verified by sequencing both strands of the insert. The polymerase chain reaction-amplified product was digested and cloned into the bacterial expression vector pT7–7 containing the *bla* gene for ampicillin resistance, under the control of the T7 RNA polymerase promoter (Tabor and Richardson, 1985). *Escherichia coli*, strain BL21(DE3), were transformed with the plasmid, and transformants were selected for ampicillin resistance. Cells were grown in M9 medium at 37°C to an A_{600} of ~0.7, induced with 1 mM isopropyl β-D-thiogalactopyranoside, and harvested after an additional 3–4 h. Lower yields of the expressed protein were recovered when the cells were grown in rich medium or to higher density before induction. The cell pellets were resuspended directly in 5 volumes of 0.4 M $HClO_4$ at 4°C and centrifuged at 30,000 × *g* for 10 min. The supernatant was neutralized with cold KOH, and precipitated $KClO_4$ was removed by centrifugation. The supernatant was dialyzed against 100 volumes of 20 mM ammonium acetate-1 mM DTT. S43C-Tβ_4 was isolated from the dialyzed supernatant by anion-exchange chromatography and reverse-phase high-performance liquid chromatography (HPLC), using the same procedure as for spleen Tβ_4, except that anion-exchange chromatography was performed in the presence of 1 mM DTT. Mass spectrometry indicated that the initiator formylmethionine residue had been cleaved off, leaving a free amino group at the N terminus. A similar mutant with a C-terminal Cys binds actin identically to Tβ_4 isolated from spleen (Carlier et al., 1996).

Glycyl endopeptidase (E.C. 3.4.22.25; papaya proteinase IV or endoproteinase Gly-C) was from Calbiochem (La Jolla, CA) or purified from papaya latex by affinity chromatography (Buttle, 1994) with equivalent results. The enzyme was activated at 37°C for 5 min with 5 mM phosphate buffer (pH 6.8), 1 mM EDTA, 5 mM cysteine before use.

Equilibrium fluorescence titrations

Equilibrium binding of Tβ_4 and actin monomers was monitored by fluorescence with a Hitachi F-2000 or a Photon Technologies International Alphascan (South Brunswick, NJ) fluorimeter at 25°C. AEDANS-actin monomers were excited at 365 nm, and the fluorescence emission was scanned from 380 to 600 nm. The peak intensity at 470 nm was used for titration analysis by least-squares fitting to the following equation:

$$FI = FI_o\text{-}(FI_o\text{-}FI_{sat}) \cdot \left(\frac{(K_d + [A] + [T]) - \sqrt{(K_d + [A] + [T])^2 - (4[A][T])}}{2[A]} \right) \quad (1)$$

where [A] and [T] are the total actin and Tβ_4 concentrations, K_d is the dissociation equilibrium constant, FI_o is the initial fluorescence intensity, and FI_{sat} is the fluorescence intensity at saturation. Floated parameters were the amplitude ($FI_o - FI_{sat}$) and the affinity (K_d). This model assumes that the fluorescence is a linear combination of bound and free states. The affinity (K_a) of unlabeled actin ($K_{unlabeled}$) for Tβ_4 was measured by competition, as described for other ligands (Huang et al., 1992; De La Cruz and Pollard, 1996), according to the relation

$$K_{unlabeled} = \frac{1 + K_{AEDANS\text{-}A}[AEDANS\text{-}A]}{[unlabeled]_{0.5}} \quad (2)$$

where $K_{AEDANS\text{-}A}$ is the association equilibrium constant for labeled actin, [AEDANS-A] is the concentration of labeled actin, and $[unlabeled]_{0.5}$ is the concentration of unlabeled actin required to displace 50% of the initially bound AEDANS-actin. Titrations in high-ionic-strength buffer were performed by measuring the fluorescence immediately after the addition of 0.1 volume of concentrated salt solutions to an equilibrated sample of actin monomers and Tβ_4 in low-ionic-strength buffer to yield the specified final ionic conditions. Spontaneous polymerization of actin monomers at the concentrations used in these measurements is slow, especially when Tβ_4 is present, and does not occur to a significant extent on this time scale.

Transient kinetics

Transient kinetic measurements were made at 25°C or at the indicated temperatures, with an Applied Photophysics SX.18MV stopped-flow spectrometer with a 1.2-ms dead time. The excitation wavelength was set at 365 nm (AEDANS measurements) or 295 nm (tryptophan fluorescence), and the emission was monitored at 90° through

400-nm (AEDANS) or 320-nm (tryptophan) long-pass interference filters. All conditions were final after mixing.

Measurements in high-ionic-strength buffer were performed by mixing equal volumes of actin monomers in low-ionic-strength buffer and a 2× salt solution to yield the final conditions stated. For association measurements, Tβ_4 in 2× salt solution was mixed with AEDANS-actin monomers in low-ionic-strength buffer. Measurements of complex dissociation were performed by mixing equal volumes of AEDANS-actin monomer solution containing a 10-fold molar excess of Tβ_4, in 2× salt, with unlabeled actin monomers in low-ionic-strength buffer. The salt was added to the actin-Tβ_4 sample immediately before loading into the stopped-flow spectrometer. Nonlinear least-squares fitting of the data was done with software provided with the instrument or with KaleidaGraph (Synergy Software).

The temperature dependence of the rates was interpreted according to the transition-state theory of absolute reaction rates (Eyring, 1935; Gutfreund, 1995), which relates the free energy of activation ($\Delta G^{\ddagger}$) of a reaction to the rate constant (k) according to

$$\Delta G^{\ddagger} = -RT \ln\left(\frac{kh}{k_B T}\right) \tag{3}$$

where h is Planck's constant, k_B is Boltzmann's constant, R is the gas constant, and T is the absolute temperature in Kelvin. The transmission coefficient is assumed to be unity and is ignored in the analysis (Gutfreund, 1995). Expanding the free energy of activation into its enthalpic ($\Delta H^{\ddagger}$) and entropic ($\Delta S^{\ddagger}$) components yields

$$\Delta H^{\ddagger} - T\Delta S^{\ddagger} = -RT \ln\left(\frac{kh}{k_B T}\right) \tag{4}$$

which can be rearranged to

$$\ln\left(\frac{kh}{k_B T}\right) = \left(\frac{-\Delta H^{\ddagger}}{R}\right)\left(\frac{1}{T}\right) + \frac{\Delta S^{\ddagger}}{R} \tag{5}$$

permitting determination of the activation enthalpy ($\Delta H^{\ddagger}$) from the slope of the line generated by plotting the left-hand side of the relation versus inverse absolute temperature. In cases where the apparent activation enthalpy varies with the temperature (i.e., Fig. 4 *A*), the slope is taken at a specified temperature. The intercept is not an accurate estimate of the activation entropy ($\Delta S^{\ddagger}$) because it is beyond the range of the data; therefore it was calculated from

$$\Delta S^{\ddagger} = \frac{\Delta H^{\ddagger} - \Delta G^{\ddagger}}{T} \tag{6}$$

Solvent manipulations

The solvent viscosity and osmotic pressure were adjusted with sucrose, glycerol, or dextran (500 kDa). Values were taken from Anderson (1970), Wolf et al. (1986), and from the Brock University osmotic stress website (http://aqueous.labs.brocku.ca/osfile.html).

The dependence of the equilibrium binding affinity on osmotic stress was interpreted, considering water as a ligand according to established thermodynamic relationships (Parsegian et al., 1995), following the relation

$$\ln(K_{eq}) = \left(\frac{-\Delta n}{55.6}\right) \times [\text{osmolal}] \tag{7}$$

where Δn is the change in number of bound water molecules obtained from the slope of the line relating $\ln(K_{eq})$ and the osmolal solute concentration.

Circular dichroism spectroscopy

Circular dichroism (CD) spectra were collected at 10°C with an Aviv 62DS CD spectropolarimeter equipped with a 1-cm-path-length Suprasil quartz cell. Spectra were obtained from 20 μM MgATP-actin in G buffer containing 0.2 mM EGTA and 0.1 mM $MgCl_2$ or 40 μM CaATP-actin in G buffer. Where specified, Tβ_4 was included at 1.1 molar equivalents and added to MgATP-actin after the cation was exchanged. Ellipticity was calculated using a molecular mass of 43 kDa for actin.

Tritium exchange

Tritium exchange experiments (Englander and Englander, 1972) were performed on ice or at 4°C. For each time point, 1 mCi [^{3}H]H_2O in 30 μl 50% sucrose (w/v) was added to 170 μl of 140 μM CaATP-actin in G-buffer. "Exchange in" was terminated after 10 min by gel filtration over Sephadex G-25 (medium) in G-buffer. Tβ_4 was added to the sample at the end of the "exchange-in" period ($t = 0$). Because the rates of interest occur on a time scale of minutes, the single-column method was used and the "exchange-out" time was varied by adjusting the flow rate and the length of the gel bed. Fractions of five drops were collected manually. Actin and [^{3}H]H_2O concentrations were determined by absorbance at 290 nm and by liquid scintillation counting, respectively. The first few protein-containing fractions had a constant [^{3}H]H_2O:protein ratio and were used to calculate the bound tritium remaining.

Cross-linking of S43C-Tβ_4 to actin

The cross-linked complex was prepared by first alkylating Cys^{374} of CaATP-actin with 1 mM *N*-ethylmaleimide at 25°C in G-buffer without DTT. The reaction was quenched after 1 h with 10 mM DTT and equimolar S43C-Tβ_4 dissolved in 3 mM triethanolamine-Cl (pH 8.0), and 1 mM DTT was added. The mixture was dialyzed exhaustively against 3 mM triethanolamine-Cl, 0.2 mM ATP, 0.2 mM $CaCl_2$, and 0.2 mM NaN_3 (pH 7.0) and diluted to 25 μM

actin-Tβ_4. Cross-linking was initiated by adding *N,N′-o*-phenylenedimaleimide (*o*PDM) freshly dissolved in dimethylformamide (DMF) to a final concentration of 0.5 mM and equilibrated for 1 h at 25°C. The final DMF concentration was ~1% (v/v). The cross-linked complex was isolated by anion-exchange chromatography, cleaved by arginine-specific digestion, and fractionated by gel filtration (Safer et al., 1997). Fractions containing the cross-linked peptide were identified based on elution volume and broadening of the 280-nm absorbance peak due to the cross-linker. A single major component was isolated from these fractions by reverse-phase HPLC on a Vydac 218TP54 C18 column (solvent A was 0.1% trifluoroacetic acid (TFA), solvent B was 0.08% TFA in acetonitrile; preparative gradient from 15 to 35% B in 60 ml at 1 ml min^{-1}).

To determine the effect of the bound metal and nucleotide on the cross-linking reaction, CaATP-actin was pretreated with NEM and converted to MgATP or MgADP-actin before S43C-Tβ_4 was added and the cross-linking reaction was initiated with *o*PDM. Cross-linked products were analyzed by sodium dodecyl sulfate-polyacrylamide gel electrophoresis (SDS-PAGE).

Proteolysis

Actin was digested with glycyl endopeptidase (4% w/w) for 10 min at 25°C with or without Tβ_4 (1.5 mol/mol actin). The reaction was stopped by alkylating the protease with 10 mM sodium iodoacetate and incubated at 25°C in the dark for 30 min. Cleavage products were analyzed by SDS-PAGE. The rate of cleavage was measured by HPLC to determine the yield of fragments.

For preparative fractionation of digests, solid guanidine-HCl was added to a final concentration of ~8 M, and alkylation was continued for 1 h. A low-molecular-weight fragment was isolated by fractionating the digests (each ~12 mg actin) by reverse-phase chromatography on a polymeric matrix (Poros R2, 50 μ; PerSeptive Biosystems) packed in a 7.5 × 250 mm column (solvent A was 0.1% TFA, solvent B was isopropanol; preparative gradient from 10 to 70% B for 60 min at 2 ml min^{-1}). A high-molecular-weight fragment that coelutes with uncleaved actin on the reverse-phase column was isolated by chromatography on hydroxyapatite (BioGel HTP, 10 × 250 mm; BioRad) in 8 M urea, eluting with a 2–30 mM sodium phosphate (pH 6.8) gradient.

Identification and characterization of peptides and fragments

Peptides were analyzed by matrix-assisted laser desorption ionization-time of flight (MALDI-TOF) mass spectroscopy and by N-terminal sequencing at the Protein Chemistry Facility of the Department of Pathology and Laboratory Medicine, University of Pennsylvania.

RESULTS

Equilibrium binding

Tβ_4 binding shifts the fluorescence emission maximum (λ_{ex} = 365 nm) of actin monomers labeled at Cys^{374} with AEDANS from 470 nm to 490 nm (Fig. 1 *A*, *inset*). The decrease in fluorescence intensity and the redshift in the emission maximum suggest an increase in polarity of the

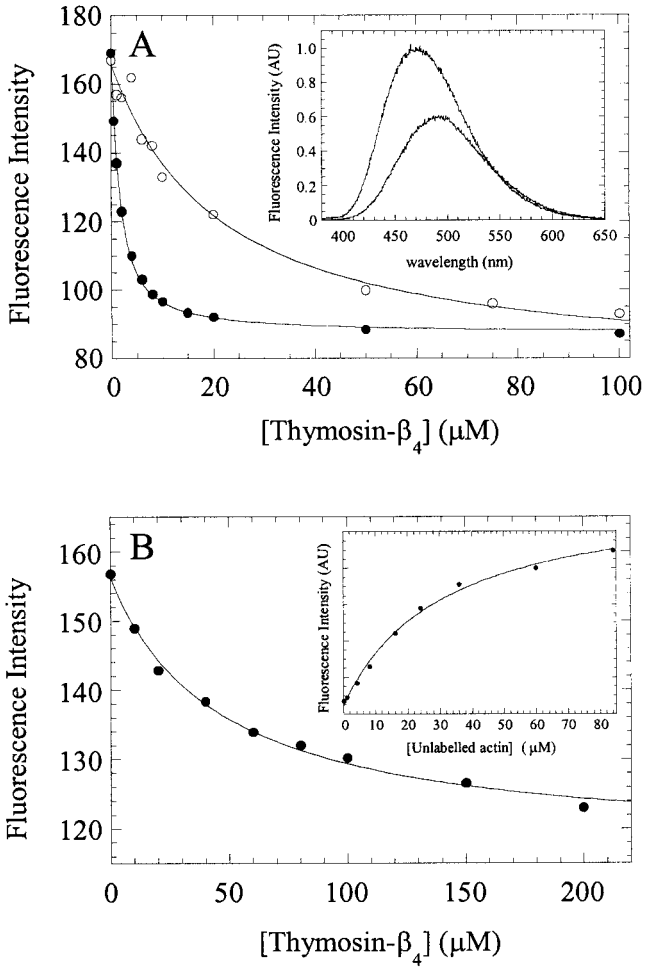

FIGURE 1 Equilibrium binding of Tβ_4 and actin monomers. (*A*) Steady-state titration of 0.5 μM MgATP AEDANS-actin in 50 (●) or 150 (○) mM KCl. Fluorescence emission intensities were recorded at 470 nm with excitation at 365 nm. The inset shows fluorescence emission scans of 1.0 μM MgATP AEDANS-actin monomers equilibrated with 0 (*left*) or 20 μM (*right*) Tβ_4. (*B*) Titration of 0.8 μM MgADP actin in 50 mM KCl. The K_d values for Tβ_4 binding to actin monomers are summarized in Table 1. The inset shows the dependence of the fluorescence of 30 μM MgATP-AEDANS-actin equilibrated with 3 μM Tβ_4 on the concentration of competing unlabeled actin. Conditions: 50 or 150 mM KCl, 1 mM $MgCl_2$, 1 mM EGTA, 0.2 mM ATP or ADP, 0.5 mM DTT, 10 mM imidazole, pH 7.0, 25°C.

TABLE 1 Summary of kinetic and equilibrium constants for Tβ4 binding to AEDANS-actin monomers at 25°C

Condition	k_{+app} ($\mu M^{-1}s^{-1}$)	k_- (s^{-1})	K_d^{kin} (μM)	K_d^{eq} (μM)
Ca-ATP (low *I*)	2.0 ± 0.1*	5.5 ± 0.8†(10)‡	2.8 ± 0.4	2.9 ± 0.2*
Ca-ATP (50 K^+/Mg^{2+})	ND	ND	ND	2.1 ± 0.1
Mg-ATP (low I)	2.5 ± 0.1	3.3 ± 0.1 (8)	1.3 ± 0.1	0.6 ± 0.1
MgATP (50 K^+/Mg^{2+})	2.1 ± 0.1	4.7 ± 0.2 (9)	2.2 ± 0.1	1.4 ± 0.1
MgATP (150 K^+/Mg^{2+})	1.1 ± 0.1	24.6 ± 1.0 (3)	22.4 ± 2.2	20.5 ± 4.3
MgADP (low *I*)	3.1 ± 0.5§	66.4 ± 9.4 (6)	ND	21.5 ± 1.2
MgADP (50 K^+/Mg^{2+})	2.0 ± 0.3§	91.5 ± 7.2 (5)	ND	44.8 ± 6.4

* Uncertainties in k_{+app} and K_d^{eq} are standard errors in the least-squares fits to the data.
† Uncertainties in k_- are ± 1 SD.
‡ (*n*) is the number of measurements from two to four preparations.
§ Calculated from $k_{+app} = k_-/K_d^{eq}$.
ND, Not determined.

AEDANS fluorophore environment, which perhaps is due to greater exposure to the solvent. We used the reduction in the fluorescence intensity at 470 nm to monitor binding (Fig. 1). Equation 1 fits the dependence of fluorescence on Tβ_4 concentration well and yields the equilibrium constant (K_d^{eq}) of the complex. The binding affinity depends on the nucleotide, cation, and ionic strength (Table 1). MgATP-actin binds the tightest. CaATP-actin binds slightly more weakly, and MgADP binds with the lowest affinity. By competition with unlabeled actin (Fig. 1 *B*, *inset*), conjugating Cys^{374} with AEDANS does not disrupt binding: K_d = 1.4 (± 0.2) μM for unlabeled versus 1.4 (± 0.1) μM for AEDANS-actin in 50 mM KCl, 1 mM $MgCl_2$ buffer.

The affinity of MgATP-actin and MgADP-actin for Tβ_4 is reduced approximately twofold with 50 mM KCl and 1 mM $MgCl_2$ (Table 1). At 150 mM KCl the apparent affinity for MgATP-actin is ~20 μM (Table 1). CaATP-actin is less sensitive to changes in ionic strength.

The extent of fluorescence quenching and the final fluorescence intensity vary with changes in the nucleotide, cation, and ionic strength. In 50 mM KCl, 1 mM $MgCl_2$ at saturation with Tβ_4 the fluorescence is quenched by 49% for MgATP-actin, 43% for CaATP-actin, and 25% for MgADP-actin; in low-ionic-strength buffers the quenching is 45% for MgATP-actin, 37% for CaATP-actin, and 24% for MgADP-actin. In agreement with Frieden (Frieden et al., 1980; Frieden and Patane, 1985), exchanging the high-affinity Ca^{2+} of AEDANS-actin (in the absence of Tβ_4) with Mg^{2+} produces an 11% fluorescence enhancement in low-ionic-strength buffer and a 6% enhancement in polymerizing buffer, and exchange of MgATP for MgADP generates a 7% quench.

Transient kinetics

The time course of fluorescence change after Tβ_4 is mixed with MgATP-AEDANS-actin monomers follows a single exponential (Fig. 2 *A*) with rates (k_{obs}) that depend linearly on the Tβ_4 concentration over a broad range (Fig. 2 *B*). There is no indication of a plateau, even at rates greater than 700 s^{-1}. The apparent second-order association rate constants (k_{+app}; K_1k_2 in Scheme 1; see first paragraph of the Discussion) obtained from the slopes of the lines have a small but significant dependence on the cation and ionic strength (Fig. 2 *B* and Table 1). By enhancement of tryptophan fluorescence (not shown), Tβ_4 binds unlabeled MgATP-actin in low-ionic-strength buffer with a comparable k_{+app} of 2.5 (± 0.2) μM^{-1} s^{-1}. Jean et al. (1994) measured rates up to 32 s^{-1} and reported a k_+ of 1.5 μM^{-1} s^{-1} at 20°C that was independent of the ionic strength.

Dissociation of the actin-Tβ_4 complex was measured directly by adding excess unlabeled actin to a sample of AEDANS-actin monomers equilibrated with Tβ_4 (Fig. 3). The effective dissociation rate constants (k_-) and the apparent equilibrium binding affinities determined from the ratio of the rate constants (K_d^{kin}) depend on the divalent cation, ionic strength, and nucleotide (Table 1). The lower affinity of Tβ_4 for CaATP-actin and MgADP-actin is due primarily, but not entirely, to a more rapid dissociation rate constant (Table 1). The affinities determined from the ratio of the rates (K_d^{kin}) are in close agreement with those obtained by equilibrium measurements (K_d^{eq}, Table 1).

Temperature dependence of rates and binding affinities

The k_{+app} for Tβ_4 binding to MgATP-actin and CaATP-actin monomers depends linearly on the inverse absolute temperature (Eyring plots, Fig. 4 *A*) over the temperature range examined (4–37°C). The activation enthalpies for Tβ_4 association ($\Delta H_a^{\ddagger}$) obtained from the slopes of the lines depend on the cation and are 11.9 (± 0.4) kcal mol^{-1} for MgATP-actin and 15.0 (± 0.4) kcal mol^{-1} for CaATP-actin (Table 2). The activation entropy for binding MgATP-actin ($T\Delta S_a^{\ddagger}$) is +0.5 kcal mol^{-1} at 25°C; CaATP-actin has an approximately sevenfold greater $T\Delta S_a^{\ddagger}$ of +3.5 kcal mol^{-1}. As a result, the free energies of activation for association ($\Delta G_a^{\ddagger}$) at 25°C are dominated by unfavorable enthalpic contributions (i.e., large positive $\Delta H_a^{\ddagger}$), even though favorable entropic (i.e., $-T\Delta S_a^{\ddagger}$ lowers $\Delta G_a^{\ddagger}$) components are

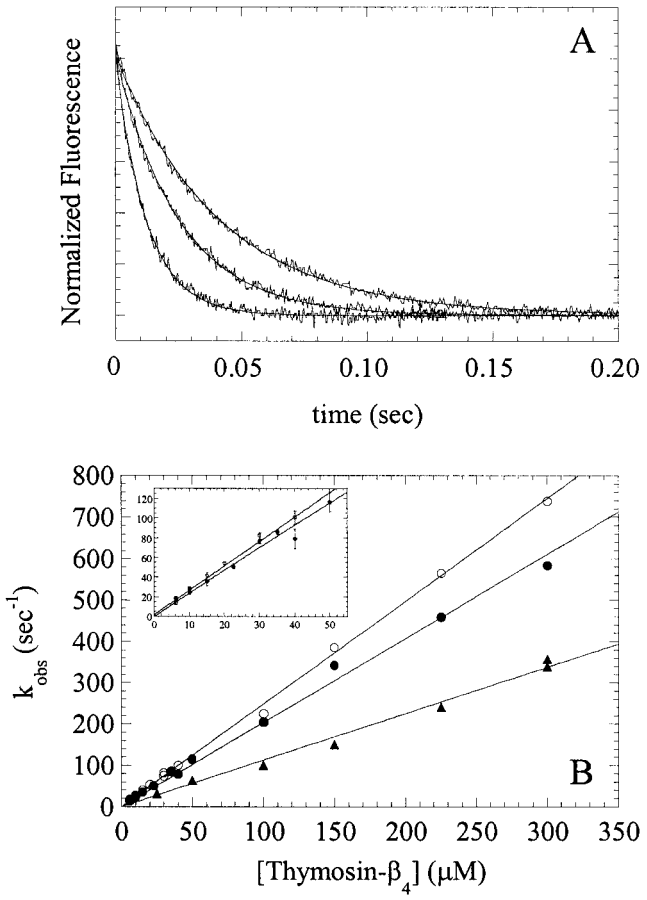

FIGURE 2 Kinetics of Tβ4 binding to MgATP-actin monomers. (*A*) Time course of fluorescence change after mixing of 0.6 μM AEDANS-MgATP-actin monomers with 35, 15, and 10 μM Tβ_4 (*left to right*) in 50 mM KCl. Fits to single exponentials (k_{obs} = 81, 40, and 24 s^{-1}) are presented as solid lines through the data. Intensities are normalized for clarity. (*B*) Dependence of k_{obs} on [Tβ_4]. ○, no KCl; ●, 50 mM KCl; ▲, 150 mM KCl. The association rate constants determined from the slopes are presented in Table 1. The inset shows the lower portion of curves. Error bars are ±1 SD of the mean from three to five determinations. Conditions: 0 (○), 50 (●), or 150 (▲) mM KCl, 1 mM $MgCl_2$, 1 mM EGTA, 0.2 mM ATP, 0.5 mM DTT, 10 mM imidazole, pH 7.0, 25°C.

present (Table 2). A positive $\Delta S_a^{\ddagger}$ suggests that solvent and possibly ions dissociate when forming the transition state.

Eyring plots for k_- (Fig. 4 *A*) also show a dependence on the cation but are distinctly nonlinear, with a minimum at ~10°C for CaATP-actin and ~14°C for MgATP-actin. At 25°C, the activation enthalpies for dissociation ($\Delta H_d^{\ddagger}$) are comparable for MgATP-actin and CaATP-actin at 16–17 kcal mol^{-1} (Table 2). The standard enthalpy changes (ΔH°_{app}) calculated from $\Delta H^{\circ}_{app} = \Delta H_a^{\ddagger} - \Delta H_d^{\ddagger}$ are −5.1 kcal mol^{-1} for MgATP-actin and −1.0 kcal mol^{-1} for CaATP-actin monomers. Entropic contributions ($-T\Delta S^{\circ}_{app}$) are −3.0 kcal mol^{-1} for MgATP-actin and −6.6 kcal mol^{-1} for CaATP-actin monomers. Therefore, the free energy of binding (ΔG°_{app}) CaATP-actin at 25°C is dominated by

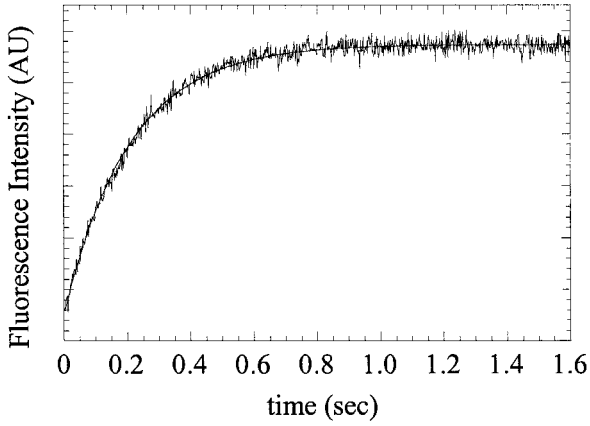

FIGURE 3 Kinetics of Tβ4 dissociation from MgATP-actin monomers: time course of fluorescence change after mixing an equilibrated mixture of 1.0 μM MgATP-AEDANS-actin and 15 μM Tβ_4 with an equal volume of 60 μM unlabeled actin. The solid line through the raw data is the fit to an exponential with a rate of 4.8 s^{-1}. Conditions: 50 mM KCl, 1 mM $MgCl_2$, 1 mM EGTA, 0.2 mM ATP, 0.5 mM DTT, 10 mM imidazole, pH 7.0, 25°C.

entropic contributions, but ΔG°_{app} for binding MgATP-actin monomers is primarily enthalpic (Table 2).

Because of the nonlinearity of Eyring plots for dissociation, van't Hoff plots for the temperature dependence of K_a^{kin} (Fig. 4 *B*) are also nonlinear. Nonlinear van't Hoff plots often result from changes in heat capacity (ΔC_p) of the reactants (Qin and Srivastava, 1998). Therefore, we used an integrated form of the van't Hoff equation (Eq. 8; Qin and Srivastava, 1998), which accounts for ΔC_p of the reacting components:

$$\ln K_a = \ln K_r + \left(\frac{\Delta H_r - T_r \Delta C_p}{R}\right)\left(\frac{1}{T_r} - \frac{1}{T}\right) + \frac{\Delta C_p}{R} \ln \frac{T}{T_r} \quad (8)$$

where T_r is an arbitrarily chosen reference temperature (25°C), and K_r and ΔH_r are the temporarily assigned association equilibrium constant and van't Hoff enthalpy, respectively, at the reference temperature. A negative ΔC_p is frequently attributed to burying of hydrophobic residues and dissociation of ordered water molecules (Creighton, 1993). The ΔC_p values for Tβ_4 binding are −0.80 kcal mol^{-1} for CaATP-actin and −0.65 kcal mol^{-1} for MgATP-actin monomers (Table 2), indicating that actin and/or Tβ_4 adopts different conformations when bound. The decrease in C_p may reflect a reduction in the amplitude or number of conformational fluctuations in the Tβ_4-actin complex. The difference between CaATP-actin and MgATP-actin suggests that alterations in monomer conformation contribute, at least partially, to the observed ΔC_p.

Viscosity, osmotic stress, and the role of bound water

The association rate constants (k_{+app}) for Tβ_4 binding to MgATP-actin (Fig. 5 *A*) and CaATP-actin (not shown) are

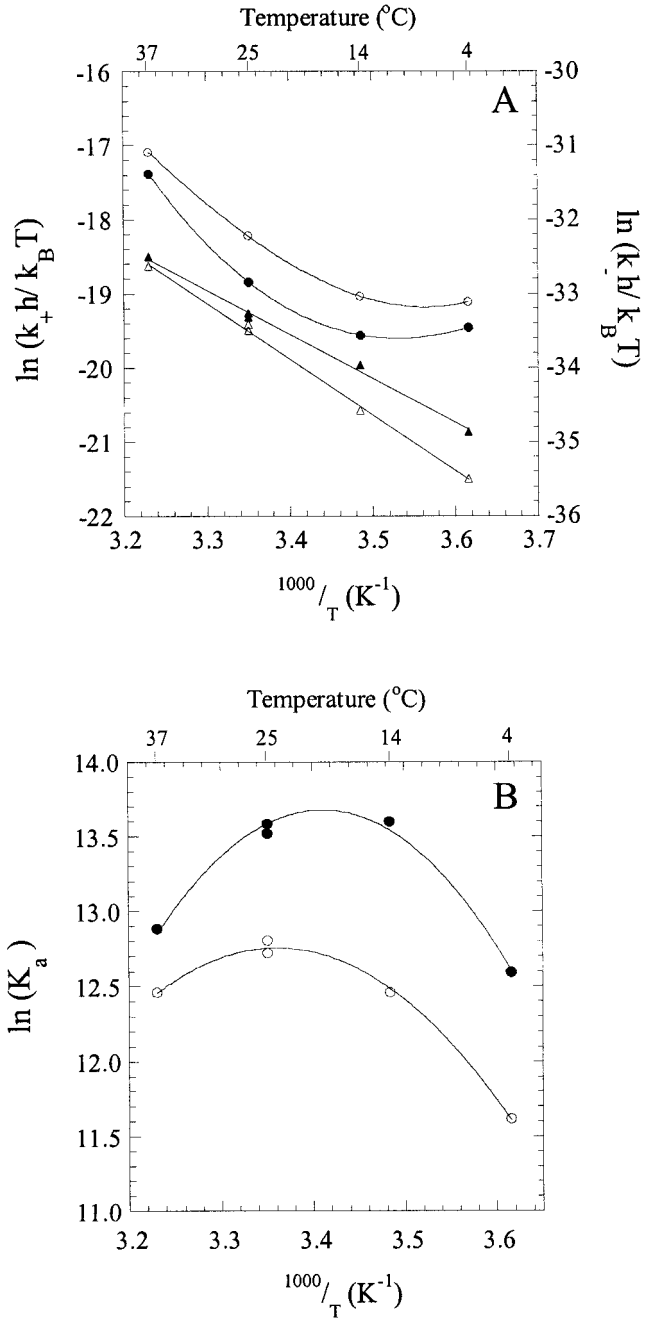

FIGURE 4 Temperature dependence of rate and equilibrium constants for Tβ4 binding. (*A*) Temperature dependence of rate constants (Eyring plots) for Tβ_4 binding to CaATP-actin (△ association, ○ dissociation) and MgATP-actin (▲ association, ● dissociation). (*B*) Temperature dependence of the equilibrium constant (van't Hoff plots) for Tβ_4 binding to CaATP-actin (○) and MgATP-actin (●). Conditions: G-buffer (CaATP) or G-buffer supplemented with 200 μM EGTA and 50 μM $MgCl_2$ (MgATP), 25°C.

independent of the solvent viscosity, indicating that it is not a diffusion-limited reaction. We used sucrose to adjust the viscosity because it does not bind most proteins (Lee and Timasheff, 1981; Wang et al., 1995). However, glycerol

TABLE 2 Thermodynamic and kinetic parameters for Tβ4 binding to MgATP- and CaATP-AEDANS-actin monomers at 25°C

Parameter*	MgATP-actin	CaATP-actin
$\Delta G_a^{\ddagger}$ (kcal mol^{-1})	11.4	11.5
$\Delta H_a^{\ddagger}$ (kcal mol^{-1})	11.9	15.0
$\Delta S_a^{\ddagger}$ (cal mol^{-1} K^{-1})	1.6	11.7
$T\Delta S_a^{\ddagger}$ (kcal mol^{-1})	0.5	3.5
$\Delta G_d^{\ddagger}$ (kcal mol^{-1})	19.5	19.1
$\Delta H_d^{\ddagger}$ (kcal mol^{-1})	17.0	16.0
$\Delta S_d^{\ddagger}$ (cal mol^{-1} K^{-1})	−8.2	−10.4
$T\Delta S_d^{\ddagger}$ (kcal mol^{-1})	−2.5	−3.1
ΔG_{app}° (kcal mol^{-1})†	−8.1	−7.6
ΔH_{app}° (kcal mol^{-1})§	−5.1	−1.0
$T\Delta S_{app}^{\circ}$ (kcal mol^{-1})¶	3.0	6.6
ΔC_p (kcal mol^{-1} K^{-1})	−0.6	−0.8

Conditions: G-buffer (CaATP) or G-buffer supplemented with 200 μM EGTA and 50 μM $MgCl_2$ (MgATP).

* Subscripts a and d refer to association and dissociation reactions, respectively.

†§¶ Calculated from $^{\dagger}\Delta G_{app}^{\circ} = \Delta G_a^{\ddagger} - \Delta G_d^{\ddagger} = RT \ln (K_d^{kin})$, $^{\S}\Delta H_{app}^{\circ} = \Delta H_a^{\ddagger} - \Delta H_d^{\ddagger}$, $^{\P}\Delta S_{app}^{\circ} = \Delta S_a^{\dagger} - \Delta S_d^{\ddagger}$.

(35% w/v), dextran (8.7% w/v), and D_2O (94% v/v) have minimal effects on the association rate constant as well (less than twofold reduction; not shown).

In contrast, dissociation of the complex (k_-) is slower at high viscosities. The inverse rate depends on the viscosity with a slope of 0.35 for MgATP-actin (Fig. 5 *A*) and 0.44 for CaATP-actin (not shown), suggesting that dissociation is partially diffusion-limited. Glycerol (35% w/v) reduced the rate by sixfold, but dextran (8.7% w/v) increased it by fourfold (not shown). D_2O (75% v/v) reduced the rate by ~30% (not shown), suggesting that solvent reorganization, binding, and ordering may influence dissociation.

The affinity of Tβ_4 for actin monomers is greater in the presence of sucrose (Fig. 5 *B*). Interpreting the dependence according to established thermodynamic principles of water activity (Eq. 5; Parsegian et al., 1995; Rand et al., 1993; Fuller and Rand, 1999) indicates that 61 (± 2) water molecules dissociate when Tβ_4 binds to MgATP-actin monomers and 72 (± 2) dissociate when Tβ_4 binds CaATP-actin. Taking a volume of 30 Å^3 for a water molecule (Rand et al., 1993), this corresponds to a decrease in volume ($-\Delta V_w$) of 1830 (± 60) Å^3 for Tβ_4-MgATP-actin and 2160 (± 60) Å^3 for Tβ_4-CaATP-actin, which is ~3–4% of the total actin monomer volume.

Tritium exchange from actin monomers is reduced by Tβ_4

Actin monomers in solution are in rapid equilibrium among multiple conformations (Tirion and ben-Avraham, 1993). Transitions among different conformational states involve local changes in the hydrogen-bonded structure of the polypeptide backbone, during which amide protons ex-

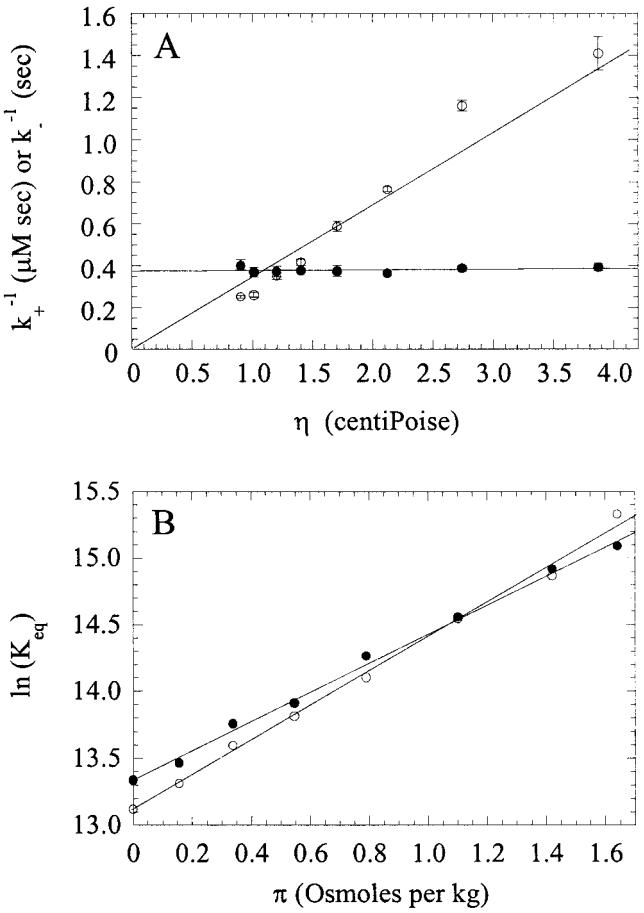

FIGURE 5 Dependence of rate and equilibrium constants for Tβ4 binding to MgATP-actin on solvent viscosity and osmotic pressure. (*A*) Dependence of (●) k_{+app} and (○) k_- on the inverse solvent viscosity. (*B*) Dependence of the equilibrium binding affinity for (●) MgATP-actin and (○) CaATP-actin monomers on osmotic pressure. Conditions: G-buffer (CaATP) or G-buffer supplemented with 200 μM EGTA and 50 μM $MgCl_2$ (MgATP). The solvent composition was adjusted with sucrose.

change with the solvent (Englander and Englander, 1972). ^{1}H-NMR can be used to study proton exchange in proteins up to 20 kDa and has been applied in a few cases to proteins up to ~30 kDa (Clore and Gronenborn, 1997). For proteins larger than ~20 kDa, overall amide hydrogen exchange rates can be measured only with tritium (Englander and Englander, 1972). Amide hydrogens in the interior of a protein that are transiently exposed exchange in tens or hundreds of seconds and can be measured manually. Solvent-exposed regions and flexible segments exchange on a subsecond time scale and are not resolved by tritium exchange methods.

$T\beta_4$ reduces the number of amide hydrogens that exchange from MgATP-actin monomers at intermediate rates (on a time scale of 100–400 s): at 100 s, actin retains 26 ^{3}H per monomer and actin-$T\beta_4$ retains 34; at 400 s actin has nine ^{3}H remaining per monomer and actin-$T\beta_4$ has 13. Thus approximately four to eight residues are locked into slower exchanging conformations in the presence of $T\beta_4$, suggesting that conformational dynamics of native actin are restricted when $T\beta_4$ is bound. This may result from dissociation of bound waters (Fig. 5 *B*), which decreases the flexibility of proteins (Fischer and Verma, 1999).

Circular dichroism spectroscopy

The near-UV CD spectrum of ATP-actin monomers depends on the cation (Fig. 6 *A*). Although MgATP-actin and CaATP-actin both yield positive ellipticity below 285 nm and negative ellipticity from 285 to 300 nm, the maxima appear at different wavelengths, CaATP-actin displays negative ellipticity below 255 nm, and the magnitude of the ellipticity is much greater for CaATP-actin than for MgATP-actin. This indicates that the electronic environments of optically active tryptophans and tyrosine residues (Murphy, 1971) are dependent on the high-affinity cation bound to actin.

$T\beta_4$ changes the spectra of both MgATP-actin and CaATP-actin (Fig. 6, *B* and *C*), but the effect is more dramatic for MgATP-actin (Fig. 6 *B*). The spectra of $T\beta_4$-MgATP-actin and $T\beta_4$-CaATP-actin are virtually indistinguishable above 280 nm. $T\beta_4$ shifts the maximum of MgATP-actin from 260 nm to that of CaATP-actin (275 nm), although the magnitude of the ellipticity is about two times lower. This indicates that the environments of the optically active chromophores and, therefore, the conformations of $T\beta_4$-MgATP-actin and $T\beta_4$-CaATP-actin in solution are different.

Cys^{43} of S43C-Tβ_4 cross-links to His^{40} of actin

The binding site of the C terminus of $T\beta_4$ on actin was identified using an engineered $T\beta_4$ construct containing a C-terminal cysteine residue (S43C-$T\beta_4$). Cross-linking with *o*PDM yields >50% complex with CaATP-actin and MgATP-actin, but the efficiency is substantially (>60%) lower with MgADP-actin because of a low affinity (Table 1) and the concentration of actin (15 μM) used in the reaction. Other cysteine-directed bifunctional cross-linkers (*p*-phenylenedimaleimide, bismaleimidomethyl ether, *m*-maleimidobenzoyl *N*-hydroxysuccinimide ester, and iodoacetic acid *N*-hydroxysuccinimide ester) give much lower yields of cross-linked product under the same conditions (data not shown).

To identify the site of cross-linking, the isolated complex was first digested with proteases that cleave actin but not $T\beta_4$, permitting chromatographic separation on the basis of size (see Experimental Procedures). The cross-linked fragment has a molecular mass of 7817 Da by mass spectrometry, as expected for S43C-$T\beta_4$ cross-linked to residues 40–62 of actin. Subsequent digestion with V8 protease generates a fragment with a mass of 2231 Da, which is the

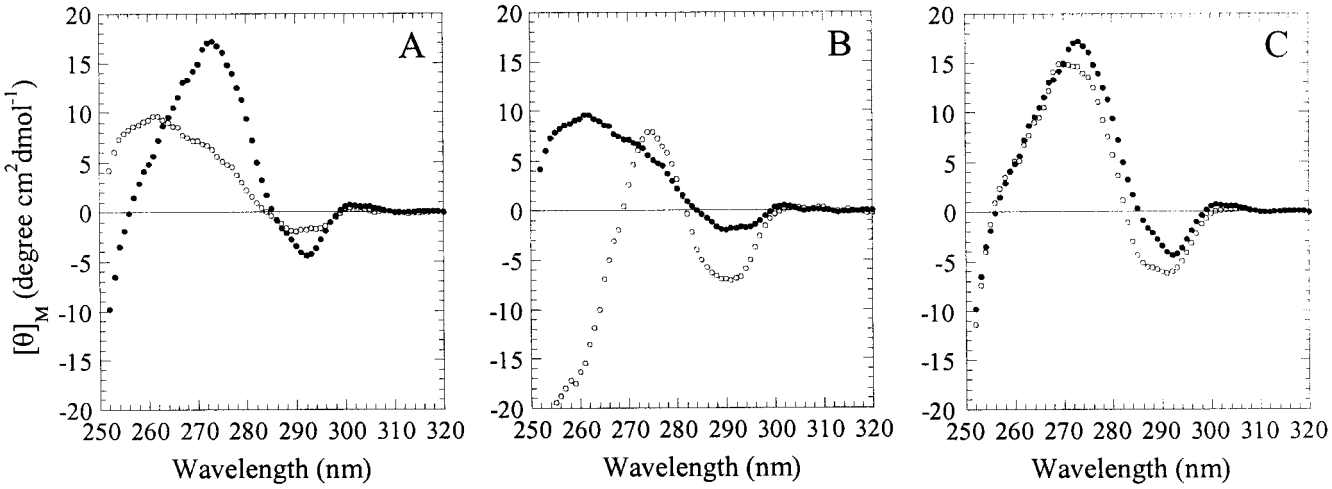

FIGURE 6 Effect of Tβ4 on the near-UV circular dichroism of actin. (*A*) CaATP-actin (●) and MgATP-actin (○) alone. (*B*) MgATP-actin (●) and Tβ_4-MgATP-actin (○). (*C*) CaATP-actin (●) and Tβ_4-CaATP-actin (○).

mass predicted for actin residues 40–51 cross-linked to residues 38–43 of S43C-Tβ_4. Cleavage of this fragment with CNBr results in a single major fragment of 1469 Da. N-terminal sequencing shows that it consists of residues 38–43 of S43C-Tβ_4 plus actin residues 40–44. The failure to detect actin His^{40} at cycle 1 and Cys^{43} of S43C-Tβ_4 at cycle 6 indicates that these are the cross-linked residues. A model for Tβ_4 binding to actin monomers based on spatial proximity of cross-linked residues is shown in Fig. 8.

FIGURE 7 Proteolysis of actin monomers by glycyl endopeptidase and isolation of cleavage products. MgATP-G-actin was digested with glycyl endopeptidase (4% w/w) for 10 min at 25°C in the absence (*lane 1*) or presence (*lane 2*) of 1.5 molar equivalents of Tβ_4. *Lane 3*: The 37-kDa fragment isolated by reverse-phase and hydroxyapatite chromatography. *Lane 4*: The 4.8-kDa fragment isolated by reverse-phase chromatography. The figure shows SDS-PAGE of products stained with Coomassie blue.

Effects of Tβ_4 on the proteolysis of actin at Gly^{46}

Glycyl endopeptidase cleaves actin but not Tβ_4, making it possible to resolve structural changes specific to actin. Cleavage is restricted to a single site on actin monomers and filaments with bound Ca^{2+} or Mg^{2+} and is not altered by Tβ_4 (Fig. 7, not shown). By mass spectrometry, the low-molecular-weight fragment has a mass of 4810 Da, corresponding to the predicted mass for actin residues 1–46. The larger fragment has a mass of 37,329 Da, as expected for actin residues 47–375. Therefore, cleavage occurs specifically at Gly^{46} in subdomain 2 of actin. N-terminal sequencing of the large fragment confirmed the cleavage site. The rate of CaATP-actin cleavage is not affected by Tβ_4 (not shown) but is >12 times more rapid for MgATP-actin (Fig. 7).

DISCUSSION

Mechanism of Tβ_4 binding to actin monomers

The most plausible mechanism defining the binding of Tβ_4 (T) and AEDANS-actin monomers (A) is

$$A^* + T \underset{k_{-1}}{\overset{k_{+1}}{\rightleftharpoons}} (A^*T) \underset{k_{-2}}{\overset{k_{+2}}{\rightleftharpoons}} AT$$

(Scheme 1)

where A* is the high-fluorescence AEDANS-actin, A is quenched, and (A*T) is the collision complex in rapid equilibrium with free A* and T. Therefore, the fluorescence change is monitoring the second transition, k_{+app} is a combination of the two reaction steps (K_1k_{+2} because $k_{+2} \gg k_{-2}$), and k_- is reporting k_{-2}. Because there is no indication of a plateau (i.e., hyperbolic dependence of k_{obs} on [Tβ_4], Fig. 2 *B*), even at rates greater than 700 s^{-1}, the sum of the

rates for the second step ($k_{+2} + k_{-2}$) must be $>2000\ s^{-1}$, and K_1 must be $>350\ \mu M$ (Fig. 2). Isomerization ($k_{+2} + k_{-2}$) may involve the ordering or folding of the collision complex, as indicated by a change in heat capacity (Table 2) and dissociation of ordered water molecules (Fig. 5 *B*), which occurs on a nanosecond time scale (Schwarz, 1965; Williams et al., 1996).

Free Tβ_4 is predominantly unstructured in solution (Czisch et al., 1993). The slow association rate constant (K_1k_2) and large (i.e., weak) K_1 for Tβ_4 binding (Table 1) suggest that only one or a few Tβ_4 conformers bind successfully to actin (Jean et al., 1994). However, given the small but significant differences in k_{+app} for CaATP-actin, MgATP-actin, and MgADP-actin (Table 1), it is likely that the conformation of actin plays an important role as well. While formation of the collision complex depends on conformational selection, the transition to the stable (low fluorescence) complex results from conformational adaptation by both Tβ_4 and actin after an encounter. The contribution of actin conformation for the stability of the complex is indicated by the nucleotide- and cation-induced changes in dissociation rates of the complexes (Table 1).

The absence of a viscosity effect on the rate of association (Fig. 5 *A*) is puzzling because one would expect the frequency of collisions, and therefore the association rate, to decrease at high viscosities. The fact that we could not detect any reduction in association rate at all viscosities examined suggests that any reduction in k_{+1} due to increased viscosity is compensated for by a decrease in k_{-1}, perhaps from a reduction in water activity (discussed below), so that there is no net effect on K_1 or K_1k_2.

The transition state and the conformation of the stable actin-Tβ_4 complex

The transition state formed from association of actin and Tβ_4 has a positive entropy of activation ($\Delta S^{\ddagger}_a$, Table 2). This is uncommon for free ligands that are coming together to form a single complex with restricted rotational and translational degrees of freedom, suggesting that solvent or perhaps weakly bound ions dissociate when forming the transition state. It is likely that these are bound to the surfaces of actin and Tβ_4 and dissociate upon encounter. The greater $\Delta S^{\ddagger}_a$ (and ΔS°, Table 2) of CaATP-actin over MgATP-actin may reflect a greater hydration of actin when Ca^{2+} is bound.

The transition state is also more ordered than the stable actin-Tβ_4 complex, as indicated by the negative $\Delta S^{\ddagger}_d$ (Table 2). This suggests that a considerable amount of dehydration occurs in forming the stable complex, as reflected in the osmotic dependence of dissociation (Fig. 5 *A*), affinity (Fig. 5 *B*), and nonlinear Eyring plot for dissociation (Fig. 4 *A*), which results from a change in heat capacity of the complex (Fig. 4 *B* and Table 2).

We propose that the dissociation of bound waters, the reduction in amide hydrogen exchange, and the inhibition of nucleotide exchange result from a closure of the nucleotide binding cleft, which is more open and hydrated in CaATP-actin than in MgATP-actin (Fuller and Rand, 1999). As a result, Tβ_4 binds weakly to MgADP-actin because the cleft is open. The more rapid dissociation and weaker binding for CaATP and MgADP (Table 1) result from a more open cleft after bound Mg^{2+} and ATP are exchanged for Ca^{2+} or ADP, making it more difficult to close the cleft and bind with high affinity. Cleft closure could occur if Tβ_4 were to insert between subdomains 1 and 2, inhibiting movement and separation of subdomains 2 and 4. There is evidence that subdomains 1 and 2 are closer to each other when MgATP is exchanged for MgADP (Kim et al., 1995), and also, but to a lesser extent when MgATP is exchanged with CaATP (Gaszner et al., 1999). This suggests that Tβ_4 dissociates rapidly from MgADP-actin (and slightly faster from CaATP-actin) because it cannot insert between the two subdomains.

The Tβ_4 binding site on actin

There are two opposing models defining the Tβ_4 binding site on actin (Reichert et al., 1996; Ballweber et al., 1997; Safer et al., 1997). Both models agree that Tβ_4 contacts the gelsolin and profilin binding sites on the barbed end of actin monomers. The differences concern the interactions at subdomain 2 of actin, where deoxyribonuclease I (DNAse I) binds. One model (Reichert et al., 1996; Ballweber et al., 1997) proposes that DNase I and Tβ_4 bind at distinct, nonoverlapping sites and that competitive binding between the two arises from negative cooperativity. This model was based on the observation that actin monomers cross-linked to Tβ_4, either through an unidentified residue (Ballweber et al., 1997) or through a spacer arm between actin Cys^{374} and residue 6 of Tβ_4 (Reichert et al., 1996), bind DNAse I. The second model (Fig. 8 in this report; Safer et al., 1997) places the thymosin binding site on subdomains 1, 2, and 3 with direct contacts at the N terminus of actin (with Lys^{18} of Tβ_4), Gln^{41} (with Lys^{38} of Tβ_4), and Glu^{167} (with Lys^{3} of Tβ_4). In this report, we show that Cys^{43} of the Tβ_4 construct, S43C-Tβ_4, cross-links specifically and efficiently to His^{40} in subdomain 2 of actin. This result is consistent with our previous model (Safer et al., 1997) and suggests that formation of a ternary complex between DNase I and cross-linked actin-Tβ_4 (Reichert et al., 1996; Ballweber et al., 1997) occurs because Tβ_4 remains tethered to the barbed end of actin monomers by the cross-link when DNAse I binds, not from cooperative structural transitions in actin.

Possible origin of the Tβ4-induced changes in the near-UV CD spectrum

Tβ_4 binding strongly affects both tryptophan and tyrosine bands in the near-UV CD spectrum of MgATP-actin (Fig.

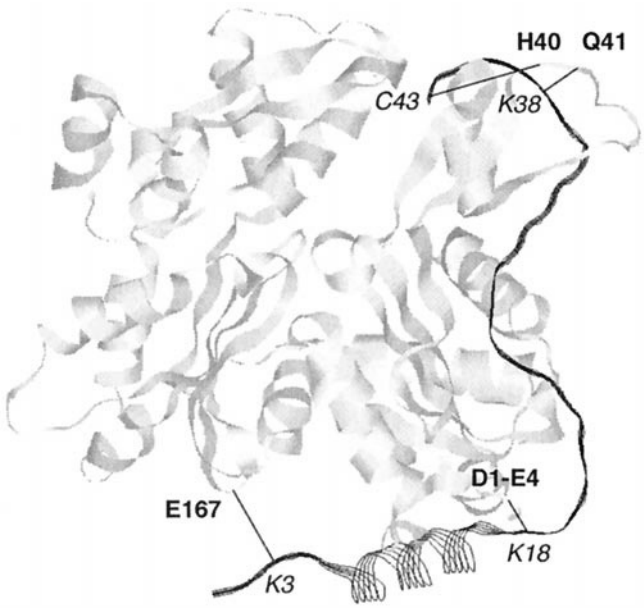

FIGURE 8 Hypothetical model of Tβ_4 binding to actin monomers based on cross-linking studies. Actin is shown as a gray ribbon; Tβ_4 is shown as black strands. Cross-links are illustrated as black lines between actin residues (*bold lettering*) and Tβ_4 residues (*labeled in italic*). Cross-link distances are not drawn to scale.

6). Changes in the CaATP-actin spectrum are less pronounced. Structural considerations implicate Tyr^{166} and Trp^{356} as the residues most likely to respond to Tβ_4 binding and contribute to the observed spectral changes: on the barbed end of actin, Tyr^{166} is adjacent to Glu^{167}, which cross-links to Tβ_4 Lys^3 (Safer et al., 1997), and Trp^{356} is near Cys^{374} and near the actin N terminus in subdomain 1 (Kabsch et al., 1990), both of which interact directly with Tβ_4. Tyr^{166} and Trp^{356} may interact directly with Tβ_4, as proposed by Safer et al. (1997), or their environments may be changed by the interaction of Tβ_4 with adjacent residues. Jean et al. (1994) proposed that the change in tryptophan fluorescence upon Tβ_4 binding was due to Trp^{356}.

Residues not at the Tβ_4 binding site may still be affected by Tβ_4 binding. We propose that Tβ_4 closes the nucleotide cleft of actin monomers, and thus an alteration in the optical activity of chromophoric residues within the cleft is expected. The most likely residues are Tyr^{306}, which directly coordinates the nucleotide (Kabsch et al., 1990), Tyr^{337}, which is adjacent to the cation, and Tyr^{69}, which is in the cleft but not coordinated with the nucleotide or cation. Tyr^{53} on subdomain 2 may also be affected because it borders the DNase-binding loop.

Implications for weak binding to actin filaments

Tβ_4 also binds actin filaments, albeit weakly (Carlier et al., 1996). Comparison of our model for the actin-Tβ_4 complex (Safer et al., 1997) with the crystallographic model for F-actin (Holmes et al., 1990) shows that only part of the binding site, at the N terminus of actin, is accessible in the filament. This should allow weak interaction between Tβ_4 and actin subunits. The remaining sites on subdomain 3 (Glu^{167}) and subdomain 2 (His^{40} and Gln^{41}) of actin are not readily accessible but may be transiently exposed as the filament experiences thermal fluctuations in shape (i.e., "breathes"). For Tβ_4 to bind stably to filaments, there must be some perturbation of the subunit contacts and, therefore, the native structure, of the filament. In principle, a positive or negative rotation in the filament twist could accommodate Tβ_4. A reduction in twist has been observed for Tβ_4-decorated filaments by electron microscopy (Carlier et al., 1996), but no high-resolution reconstruction is available. We propose that the perturbation results from accommodating Tβ_4 and that the binding affinity is weak for filaments because most of the binding site is not accessible. An inaccessible site should yield a slow association rate constant for filament binding, as with phalloidin (De La Cruz and Pollard, 1996).

EMDLC is a Burroughs-Wellcome Fund Fellow of the Life Sciences Research Foundation. This research was supported by National Institutes of Health Grants AR40840 to DS, GM57247 to EMO, and AR35661 to HLS.

REFERENCES

Anderson, N. G. 1970. *In* CRC Handbook of Biochemistry, Selected Data for Molecular Biology, 2nd Ed. H. A. Sober, editor. CRC Press, Boca Raton, FL. J288–J291.

Ballweber, E., E. Hannappel, T. Huff, and H. G. Mannherz. 1997. Mapping the binding site of thymosin β_4 on actin by competition with G-actin binding proteins indicates negative co-operativity between binding sites located on opposite subdomains of actin. *Biochem. J.* 327:787–793.

Barden, J. A., and C. G. dos Remedios. 1985. Conformational changes in actin resulting from Ca^{2+}/Mg^{2+} exchange as detected by proton NMR spectroscopy. *Eur. J. Biochem.* 146:5–8.

Buttle, D. J. 1994. Glycyl endopeptidase. *Methods Enzymol.* 244:539–555.

Carlier, M.-F., D. Didry, I. Erk, J. Lepault, M. L. Van Troys, J. Vandekerckhove, I. Perelroizen, H. Yin, Y. Doi, and D. Pantaloni. 1996. Tβ_4 is not a simple G-actin sequestering protein and interacts with F-actin at high concentrations. *J. Biol. Chem.* 271:9231–9239.

Carlier, M.-F., C. Jean, K. J. Rieger, M. Lenfant, and D. Pantaloni. 1993. Modulation of the interaction between G-actin and thymosin β_4 by the ATP/ADP ratio: possible implication in the regulation of actin dynamics. *Proc. Natl. Acad. Sci. USA.* 90:5034–5038.

Carlier, M.-F., D. Pantaloni, and E. D. Korn. 1986. Fluorescence measurements of the binding of cations to high-affinity and low-affinity sites on ATP-G-actin. *J. Biol. Chem.* 261:10778–10784.

Chik, J. K., U. Lindberg, and C. E. Schutt. 1996. The structure of an open state of beta-actin at 2.65 Å resolution. *J. Mol. Biol.* 263:607–623.

Clore, G. M., and A. M. Gronenborn. 1997. NMR structures of proteins and protein complexes beyond 20,000 M_r. *Nature Struct. Biol.* 4:849–853.

Czisch, M., M. Schleicher, S. Horger, W. Voelter, and T. A. Holak. 1993. Conformation of thymosin β_4 in water determined by NMR spectroscopy. *Eur. J. Biochem.* 218:335–344.

De La Cruz, E. M., and T. D. Pollard. 1996. Kinetics and thermodynamics of phalloidin binding to actin filaments from three divergent species. *Biochemistry.* 35:14054–14061.

Englander, S. W., and J. J. Englander. 1972. Hydrogen-tritium exchange. *Methods Enzymol.* 26:406–413.

Eyring, H. 1935. The activated complex and the absolute rate of chemical reactions. *Chem. Rev.* 17:65–77.

Fischer, S., and C. S. Verma. 1999. Binding of buried structural water increases the flexibility of proteins. *Proc. Natl. Acad. Sci. USA.* 96: 9613–9615.

Frieden, C., D. Lieberman, and H. R. Gilbert. 1980. A fluorescent probe for conformational changes in skeletal muscle G-actin. *J. Biol. Chem.* 255: 8991–8993.

Frieden, C., and K. Patane. 1985. Differences in G-actin containing bound ATP or ADP: the Mg^{2+}-induced conformational change requires ATP. *Biochemistry.* 24:4192–4196.

Fuller, N., and R. P. Rand. 1999. Water in actin polymerization. *Biophys. J.* 76:3261–3266.

Gaszner, B., M. Nyitrai, N. Hartvig, T. Koszegi, B. Somogyi, and J. Belagyi. 1999. Replacement of ATP with ADP affects the dynamic and conformational properties of actin monomer. *Biochemistry.* 38: 12885–12892.

Goldschmidt-Clermont, P.-J., M. I. Furman, D. Wachsstock, D. Safer, V. T. Nachmias, and T. D. Pollard. 1992. The control of actin nucleotide exchange by thymosin β_4 and profilin: a potential regulatory mechanism for actin polymerization in cells. *Mol. Biol. Cell.* 3:1015–1024.

Gutfreund, H. 1995. Kinetics for the Life Sciences. Cambridge University Press, Cambridge, UK.

Hannappel, E., and F. Wartenberg. 1993. Actin-sequestering ability of thymosin β_4, thymosin β_4 fragments, and thymosin β_4-like peptides as assessed by the DNase I inhibition assay. *Biol. Chem. Hoppe-Seyler.* 374:117–122.

Heintz, D., A. Reichert, M. Mihelic, W. Voelter, and H. Faulstich. 1993. Use of bimanyl actin derivative (TMB-actin) for studying complexation of β-thymosins. Inhibition of actin polymerization by thymosin β_9. *FEBS Lett.* 329:9–12.

Holmes, K. C., D. Popp, W. Gebhard, and W. Kabsch. 1990. Atomic model of the actin filament. *Nature.* 347:44–49.

Houk, T. W., and K. Ue. 1974. The measurement of actin concentration in solution: a comparison of methods. *Anal. Biochem.* 62:66–74.

Huang, Z., R. P. Haugland, W. M. You, and R. P. Haugland. 1992. Phallotoxin and actin binding assay by fluorescence enhancement. *Anal. Biochem.* 200:199–204.

Huff, T., D. Zerzawy, and E. Hannappel. 1995. Interactions of beta-thymosins, thymosin beta 4-sulfoxide, and N-terminally truncated thymosin beta 4 with actin studied by equilibrium centrifugation, chemical cross-linking and viscometry. *Eur. J. Biochem.* 230:650–657.

Jean, C., K. Rieger, L. Blanchoin, M.-F. Carlier, M. Lenfant, and D. Pantaloni. 1994. Interaction of G-actin with thymosin β_4 and its variants thymosin β_9 and thymosin β_9^{met}. *J. Muscle Res. Cell Motil.* 15:278–286.

Kabsch, W., H.-G. Mannherz, D. Suck, E. F. Pai, and K. C. Holmes. 1990. Atomic structure of the actin:DNase I complex. *Nature.* 347:37–44.

Kim, E., M. Motoki, K. Seguro, A. Muhlrad, and E. Reisler. 1995. Conformational changes in subdomain 2 of G-actin: fluorescence probing by dansyl ethylenediamine attached to Gln-41. *Biophys. J.* 69: 2024–2032.

Kinosian, H. J., L. A. Selden, J. E. Estes, and L. C. Gershman. 1993. Nucleotide binding to actin. Cation dependence of nucleotide dissociation and exchange rates. *J. Biol. Chem.* 268:8683–8691.

Laemmli, U. K. 1970. Cleavage of structural proteins during the assembly of the head of bacteriophage T4. *Nature.* 227:680–685.

Lee, J. C., and S. N. Timasheff. 1981. The stabilization of proteins by sucrose. *J. Biol. Chem.* 256:7193–7201.

Lehrer, S. S., and G. Kerwar. 1972. Intrinsic fluorescence of actin. *Biochemistry.* 11:1211–1217.

MacLean-Fletcher, S., and T. D. Pollard. 1980. Identification of a factor in conventional muscle actin preparations which inhibits actin filament self-association. *Biochem. Biophys. Res. Commun.* 96:18–27.

McLaughlin, P. J., J. T. Gooch, H.-G. Mannherz, and A. G. Weeds. 1993. Structure of gelsolin segment-1 actin complex and the mechanism of filament severing. *Nature.* 364:685–692.

Moraczewska, J., H. Strzelecka-Golaszewska, P. D. J. Moens, and C. G. dos Remedios. 1996. Structural changes in subdomain 2 of G-actin observed by fluorescence spectroscopy. *Biochem. J.* 317:605–611.

Murphy, A. J. 1971. Circular dichroism of the adenine and 6-mercaptopurine nucleotide complexes of actin. *Biochemistry.* 10:3723–3728.

Pardee, J. D., and J. A. Spudich. 1982. Purification of muscle actin. *Methods Enzymol.* 85:164–181.

Parsegian, V. A., R. P. Rand, and D. C. Rau. 1995. Macromolecules and water: probing with osmotic stress. *Methods Enzymol.* 259:43–94.

Pollard, T. D. 1984. Polymerization of ADP actin. *J. Cell Biol.* 99: 769–777.

Qin, L., and D. K. Srivastava. 1998. Energetics of two-step binding of a chromophoric reaction product, *trans*-3-indoleacryloyl-CoA, to medium-chain acyl- coenzyme-A dehydrogenase. *Biochemistry.* 37: 3499–3508.

Rand, R. P., N. L. Fuller, P. Butko, G. Francis, and P. Nicholls. 1993. Measured change in protein solvation with substrate binding and turnover. *Biochemistry.* 32:5925–5929.

Reichert, A., D. Heintz, H. Echner, W. Voelter, and H. Faulstich. 1996. The ternary complex of DNase I, actin, and thymosin β_4. *FEBS Lett.* 387:132–136.

Reichert, A., D. Heintz, W. Voelter, M. Mihelic, and H. Faulstich. 1994. Polymerization of actin from the thymosin β_4 complex initiated by the addition of actin nuclei, nuclei stabilizing agents or myosin S1. *FEBS Lett.* 347:247–250.

Safer, D., T. R. Sosnick, and M. Elzinga. 1997. Thymosin β_4 binds actin in an extended conformation and contacts both the barbed and pointed ends. *Biochemistry.* 36:5806–5816.

Schutt, C. E., J. C. Myslik, M. D. Rozycki, N. C. W. Goonesekere, and U. Lindberg. 1993. The structure of crystalline profilin-β-actin. *Nature.* 365:810–816.

Schwarz, G. 1965. On the kinetics of the helix-coil transition of polypeptides in solution. *J. Mol. Biol.* 11:64–67.

Strzelecka-Golaszewska, H., J. Moraczewska, S. Y. Khaitlina, and M. Mossakowska. 1993. Localization of the tightly bound divalent-cation-dependent and nucleotide-dependent conformation changes in G-actin using limited proteolytic digestion. *Eur. J. Biochem.* 211:731–742.

Tabor, S., and C. C. Richardson. 1985. A bacteriophage T7 RNA polymerase/promoter system for controlled exclusive expression of specific genes. *Proc. Natl. Acad. Sci. USA.* 82:1074–1078.

Tirion, M. M., and D. ben-Avraham. 1993. Normal mode analysis of G-actin. *J. Mol Biol.* 230:186–195.

Vinson, V. K., E. M. De La Cruz, H. N. Higgs, and T. D. Pollard. 1998. Interactions of *Acanthamoeba* profilin with actin and nucleotides bound to actin. *Biochemistry.* 37:10871–10880.

Wang, A., A. D. Robertson, and D. W. Bolen. 1995. Effects of a naturally occurring compatible osmolyte on the internal dynamics of ribonuclease A. *Biochemistry.* 34:15096–15104.

Weber, A., V. T. Nachmias, C. R. Pennise, M. Pring, and D. Safer. 1992. Interaction of thymosin β_4 with muscle and platelet actin: implications for actin sequestration in resting platelets. *Biochemistry.* 31:6179–6185.

Williams, S., T. P. Causgrove, R. Gilmanshin, K. S. Fang, R. H. Callendar, W. H. Woodruff, and R. B. Dyer. 1996. Fast events in protein folding: helix melting and formation in a small peptide. *Biochemistry.* 35: 691–697.

Wolf, A. V., M. G. Brown, and P. C. Prentiss. 1986. *In* CRC Handbook of Chemistry and Physics. R. T. Weast, editor. CRC Press, Boca Raton, FL. D219, D262.

Yu, F.-X., S.-C. Lin, M. Morrison-Bogorad, M. A. L. Atkinson, and H. L. Yin. 1993. Thymosin β_{10} and thymosin β_4 are both actin monomer sequestering proteins. *J. Biol. Chem.* 268:502–509.